



Effect of deformation mode, dynamic recrystallization and twinning on rolling texture evolution of AZ31 magnesium alloys

Li-li GUO¹, Fumio FUJITA²

1. Engineering Research Center of Continuous Extrusion, Dalian Jiaotong University, Dalian 116028, China;
2. Department of Metallurgy, Graduate School of Engineering, Tohoku University, Aoba, Sendai, 980-8579, Japan

Received 20 March 2017; accepted 18 September 2017

Abstract: In order to obtain quantitative relationship between (0002) texture intensity and hot rolling conditions, conventional rolling experiments on AZ31 magnesium alloys were performed with 20%–40% reductions and temperatures within the range of 300–500 °C. Shear strain and equivalent strain distributions along the thickness of the rolled sheets were calculated experimentally using embedded pin in a rolling sheet. Rolling microstructures and textures in the sheet surface and center layers of the AZ31 alloys were measured by optical microscopy (OM), X-ray diffractometry (XRD) and electron back scatter diffraction (EBSD). Effects of the rolling strain, dynamic recrystallization (DRX) and twinning on the texture evolution of the AZ31 alloys were investigated quantitatively. It is found that the highest (0002) basal texture intensities are obtained at a starting rolling temperature of 400 °C under the same strain. Strain–temperature dependency of the (0002) texture intensity of the AZ31 alloy is derived.

Key words: magnesium alloy sheet; hot rolling; texture; dynamic recrystallization; twinning

1 Introduction

Magnesium and its alloys have considerable potential as structural materials in various industrial fields, such as automobile and electronic products [1]. However, these metals have not yet been fully developed because of their limited cold formability and ductility. The poor cold formability of existing magnesium alloys is mainly caused by their strong basal texture [2], because basal texture induces high normal anisotropy in a sheet and increases the difficulty in deformation accompanied by thickness reduction. This characteristic remarkably restricts the applications of these alloys in the form of sheets [3–5].

It is well known that shear deformation can modify (0001) basal texture. Normal rolling includes two deformation modes, namely, compression and shear. The compression strain is uniform along the sheet thickness direction. The shear strain is the largest on the sheet surface but zero at the sheet center. Consequently, deformation modes lead to different textures at various thickness locations of rolled sheet. However, some studies on texture evolution during rolling are

characterized by the absence of deformation mode and quantitative rolling strain [6,7]. On the other hand, rolling temperature is another important parameter that can influence the textural evolution in AZ31 alloys. High rolling temperature has a remarkable effect on weakening the basal texture intensity [5]. The weakening of the basal texture at high temperature deformation has been suggested to be caused by dynamic recrystallization (DRX) or rotational dynamic recrystallization (RDRX) [8,9]. Nevertheless, these rolling tests are conducted in multi-passes with different reductions per pass, resulting in differences not only in the strain but also in the rolling temperature at various sheet thickness locations. Consequently, various temperatures and strain conditions lead to different DRX microstructures which may influence the microtextural evolution. Weakening the (0002) basal texture intensity and improving grain refinement by DRX during hot rolling process are some of the main purposes. However, little information is available under the quantitative rolling conditions required to obtain controlled texture in AZ31 alloy during hot rolling process.

In this study, in order to examine the quantitative relationship between the basal texture intensity and the

hot rolling conditions, finite difference (FD) simulations were used to estimate the rolling strain and temperature distributions in the sheet thickness direction [10]. Normal rolling experiments were conducted in a wide range of temperatures and strains. Moreover, the effects of deformation mode, DRX, and twinning on the texture evolution of AZ31 alloy during hot rolling process were investigated.

2 Methods of experiment and calculation

2.1 Experimental method

An as-cast magnesium alloy pin with a diameter of 2.8 mm was embedded into the mid-width location of sheets with the central axis parallel to the normal direction (ND) to evaluate the shear strain distribution through the sheet thickness [11]. Starting sheets of magnesium alloys (5.6 mm in thickness, 40 mm in width, and 150 mm in length) were used in the present study. The sheets had a typical rolling texture with the *c*-axis lying parallel to the ND. The starting sheets were held for 30 min at 300, 350, 400, 450, and 500 °C in an electric furnace. Then, normal rolling was conducted at different reductions of approximately 22%, 30%, 35%, and 39% in one pass, as mentioned in previous studies [11].

The specimens for the OM, XRD, and EBSD

examinations were cut from the center of the rolled sheets. Digital microscopes (Keyence) and VHX-900 and VH-5000 software were used for microstructural analysis. Specimens for EBSD measurement were electropolished in HNO₃ solution. Measurements were taken at two different locations (center and surface locations) in the transverse direction (TD) plane. The areas, all 200 μm in length in the ND and 150 μm in width in the rolling direction (RD), were automatically scanned with a step size of 0.8 μm for all specimens using TSL OIM (orientation imaging microscopy) Data Collection Ver. 5.31 in Philips XL30-FEG-SEM. X-ray texture analysis was performed using the Schulz reflection method to obtain an incomplete (0002) pole figure and texture intensities using Rigaku RINT2000. The measurements were made with a Rigaku diffractometer using Cu K_α radiation at 40 kV and 100 mA, and conducted in the surface planes along the thickness direction.

2.2 Strain calculation

The optical micrographs of the embedded pin interface and its inclination distributions rolled at various reductions and 300 °C are shown in Fig. 1. The pin, embedded perpendicularly to the ND plane before rolling, was sheared towards RD after one pass rolling at each rolling reduction. Then, the angle of the pin inclination

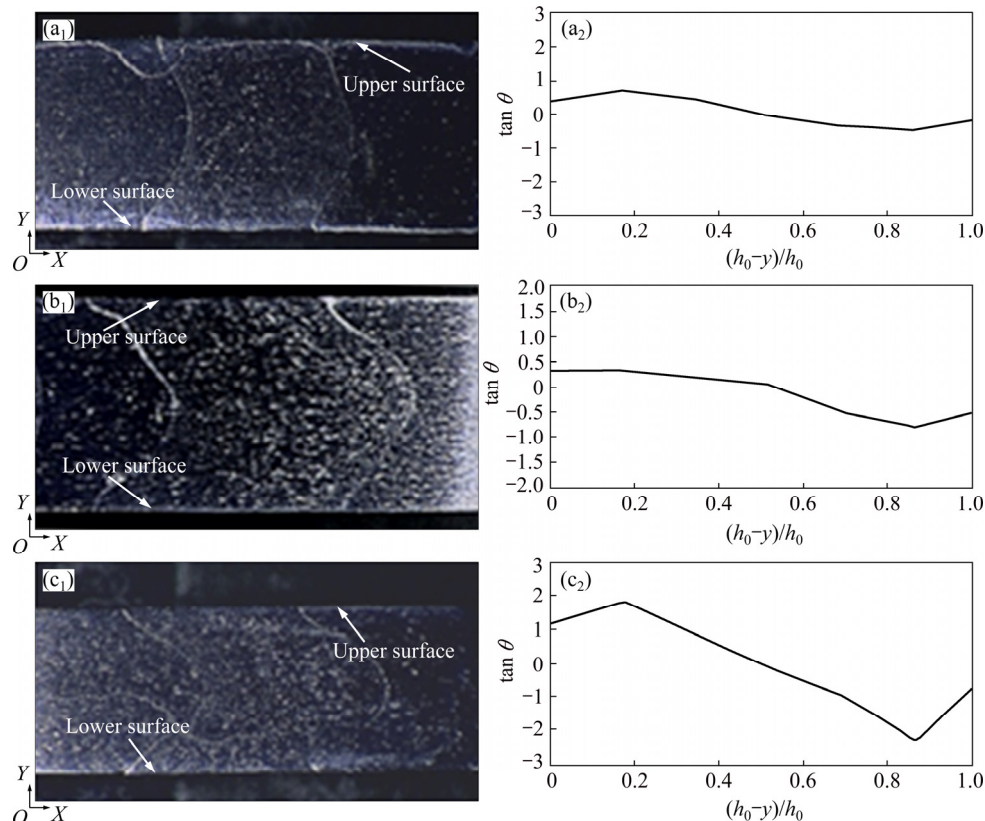


Fig. 1 OM images of embedded pin interface and average $\tan \theta$ after one pass rolling at 300 °C and different rolling reductions: (a₁, a₂) 21.9%; (b₁, b₂) 29.1%; (c₁, c₂) 36.2%

($\tan \theta$) was calculated from the x and y coordinates of the contour lines, which were smoothed by least square method, as shown in Figs. 1(a₂), (b₂) and (c₂). From the thickness values of the initial material (h_0), the rolled sheet (h_{out}), and the angle of the pin inclination ($\tan \theta$), the total reduction shear strain (γ) was calculated based on the rolling theories by integrating the shear strain in the roll bite. The distributions of the shear strain (γ) and equivalent strain ($\bar{\varepsilon}_{eq}$) were calculated by Eqs. (1) and (2) [10].

The redundant shear strain was calculated as follows:

$$\gamma = \gamma_1 + \gamma_2 = \int_0^{x_{n1}} \alpha \left(\frac{2x}{Rh} \right) dx + \int_{x_{n1}}^{x_n} \alpha \left(\frac{2x}{Rh} \right) dx = \alpha \ln \left(1 + \frac{x_n^2}{Rh_{out}} \right) \quad (1)$$

where γ_1 and γ_2 are the redundant shear strains before and after the neutral point within the roll bite, h is the height of the rolled sheet in the roll bite, R is the radius of the roll, x_n is the length of the roll bite, x_{n1} is the position of neutral point in the roll bite, α is a ratio of the redundant shear strain to the compression strain and is represented by the rolling parameters as follows:

$$\alpha = \tan \theta \cdot R \cdot h_{out}^2 [h_{out} (x_n^2 - 2x_{n1}^2) + \frac{1}{2R} (x_n^4 - 2x_{n1}^4)]^{-1} \quad (2)$$

The equivalent strain ($\bar{\varepsilon}_{eq}$) under the plane strain condition is simply expressed as follows:

$$\bar{\varepsilon}_{eq} = \frac{\sqrt{2}}{3} \sqrt{6\varepsilon_c^2 + 1.5\gamma^2} \quad (3)$$

where ε_c is the compression strain.

The equivalent strain and redundant shear strain distributed in the sheet thickness under different rolling conditions (rolling temperature and reductions) were successfully measured by the method stated above. The changes in the equivalent and shear strains with reduction ratio of the near-surface layer ($h/h_0=0.15$) and the center layer ($h/h_0=0.5$) in the sample rolled at 300 °C are shown in Fig. 2. The redundant shear strain of the center layer is almost zero, and slight change in this strain is observed with changes in the reduction ratio. By contrast, redundant shear strain near the surface layer shows the highest strain at each rolling reduction and increases more quickly as the rolling reduction rises. The equivalent strain of the near-surface layer also increases sharply compared with that at the center layer.

3 Results and discussion

3.1 Texture evolution in different deformation modes

The (0002) and (10 $\bar{1}$ 0) pole figures in the surface and center layers of AZ31 alloys rolled at various

reductions and 300 °C are shown in Fig. 3. The basal plane (0002) is parallel to the normal plane of the rolled sheet, and the $\langle 11\bar{2}0 \rangle$ direction is aligned perpendicularly to the RD in the center layer rolled at 300 °C and 36% reduction. The following differences are found between the surface and center layers:

1) In the surface layer, the (0002) texture of samples rolled under different reductions shows basal poles inclined at 5°–15° toward the RD. These results are consistent with those reported in the literatures. This phenomenon is considered to be related to the shear deformation [12]. In the center layer, double peak textures appear at $\pm(10^\circ-15^\circ)$ along the RD in the samples rolled with large reductions (29.1% and 36.2%). However, in the 22% rolled sample, the (0002) basal texture shows a single-peak texture similar to that of the surface layer. Here, a symmetrical splitting of the (0002) basal is the main feature of texture in the center layer at 300 °C rolling.

2) In addition, the (0002) basal texture intensity increases significantly in the surface layer with the rolling reduction, contrary to its slight decreasing in the center layer.

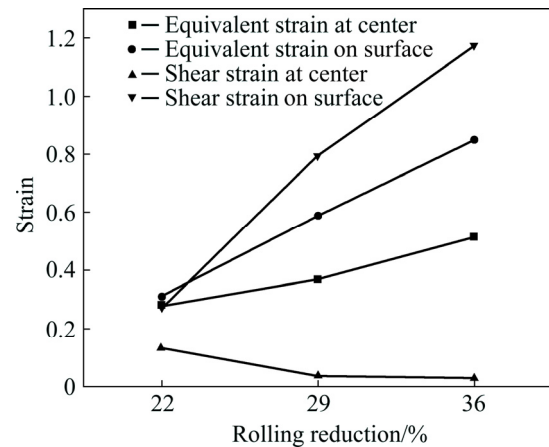


Fig. 2 Variation of equivalent strain and shear strain with reductions of AZ31 sheets rolled at 300 °C

Figure 4 illustrates the lattice rotation under three different deformation modes, namely, uniaxial compression in Fig. 4(a), planar strain compression in Fig. 4(b), and a combination of the planar strain compression and redundant shear in Fig. 4(c). Figure 4(a) shows the lattice rotation in the simplest model of a single crystal. We draw the initial basal plane with an inclination of approximately 45° with respect to the compression axis. When the compression stress acts on the object, the rotation of the normal slip plane is toward a position with the c -axis parallel to the compression axis, according to the rotation principle for a single crystal lattice [13]. However, grains in the polycrystalline material present various orientations, as shown in the left

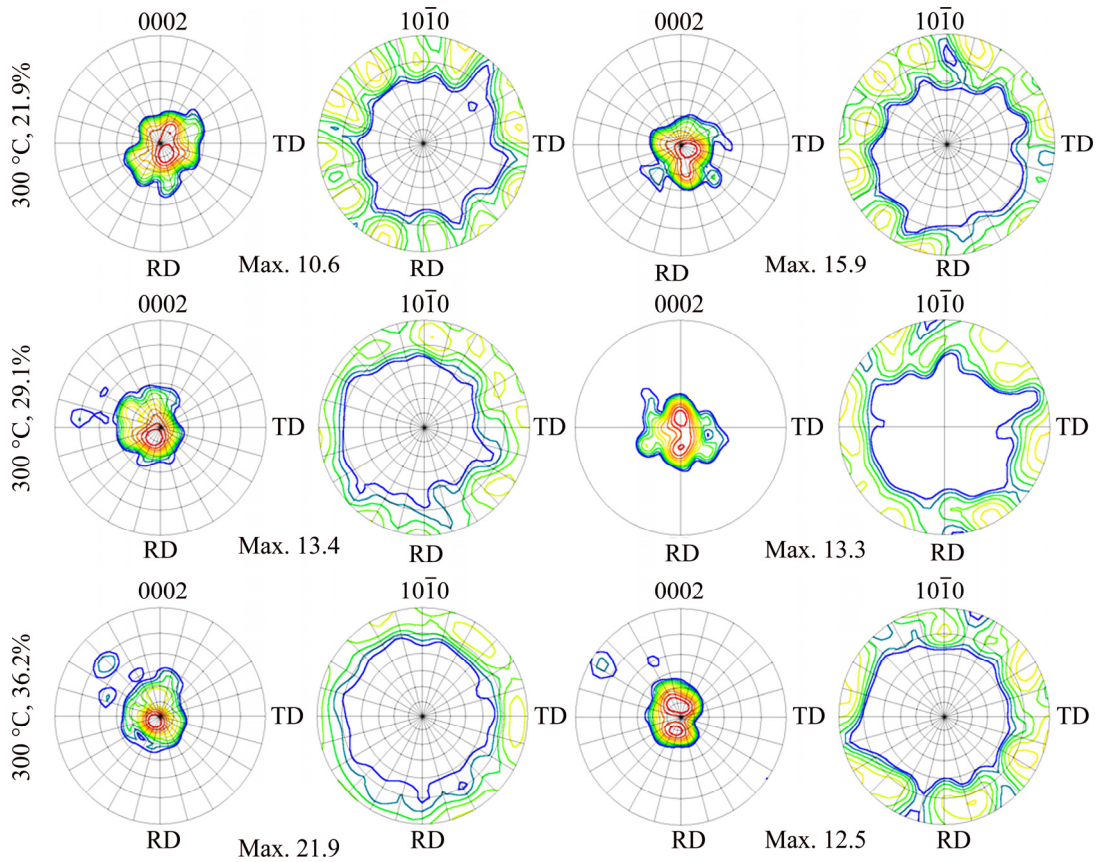


Fig. 3 (0002) and (10 $\bar{1}0$) pole figures of AZ31 alloys rolled at 300 °C with various reductions, measured in surface and center layers

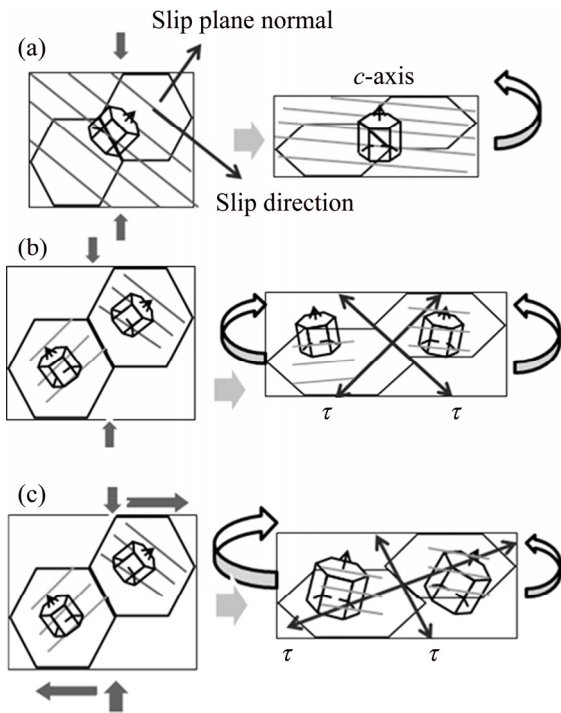


Fig. 4 Schematic illustration of lattice rotation under three different types of deformation modes: (a) Uniaxial compression; (b) Planar strain compression; (c) Planar strain compression combined with redundant shear

hand of Fig. 4(b). The maximum shear stress occurs in the symmetrical direction of 45° with respect to the compression axis (right hand of Fig. 4(b)), because the sheet center layer is under planar strain compression. This kind of shear stress causes the random distribution grains in the center layer to rotate simultaneously towards the same direction (ND) from two sides when the basal slip operates. Here, we assume that all grains in the center layer rotate finally to the direction in which the *c*-axis is parallel to the compression axis. Further deformation may not continue under this condition, because Schmid factors of basal slip are almost zero in this orientation. Therefore, many slip planes apparently become stabilized at this symmetric orientation, as shown in the right hand of Fig. 4(b). Moreover, AGNEW et al [14] demonstrated in their simulation study that double twins and increased activity of the non-basal $\langle c+a \rangle$ slip mode may result in the double-peak texture. Similarly, a third case is considered, which consists of not only the planar strain compression but also the redundant shear stress. The direction of the maximum shear stress under such stress state is changed away from 45° symmetric orientation to the shear direction. Hence, the redundant shear changes the direction of the main

shear stresses in the surface layer of rolled sheets (right hand of Fig. 4(c)). Consequently, grains of the surface layer rotate towards RD by rigid rotations. A simulation study verified that this shear component could considerably change the orientation of the grains and the stability characteristics of texture in pure magnesium during asymmetric rolling [15].

3.2 Effect of rolling temperature on (0002) rolling texture

FD simulation was used in the previous study to show that, although the temperature of the sheet surface is decreased by over 100 °C during the journey from the entrance to the exit, few differences in rolling temperature history may be observed in the same thickness layer when sheets are heated to the same starting rolling temperature but rolled at different thickness reductions [11]. Therefore, the starting rolling temperature can be used here. XRD is used to measure the macrot texture to obtain the accurate values of (0002) texture intensity. Figure 5 presents the (0002) incomplete pole figures of the surface layers of AZ31 sheets rolled at 300–500 °C under various reductions. Maximum intensity values are shown in each pole figure. All (0002) basal planes align parallel to the RD–TD plane. The (0002) pole spreads slightly to RD at 300 °C, 350 °C and each strain level, but this pole spreads to TD at 450 °C and large strain level. The maximum (0002) basal texture intensity changes with the increase of starting rolling temperature and equivalent strain. The (0002) pole

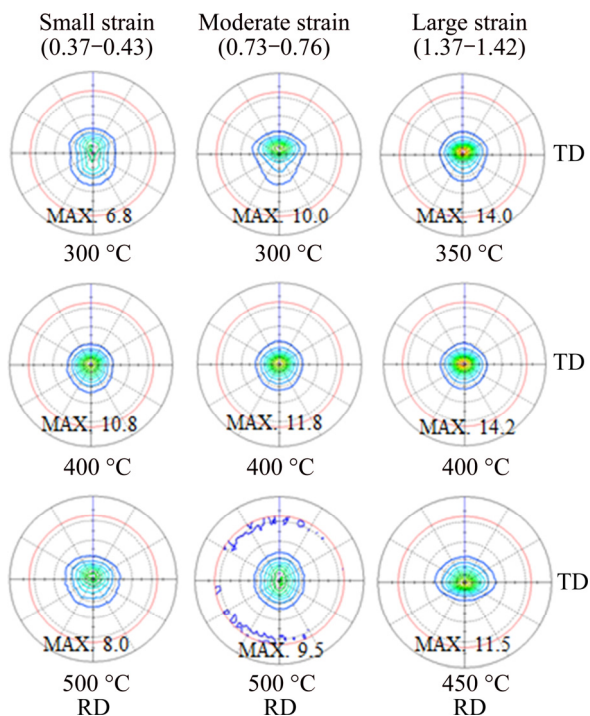


Fig. 5 (0002) incomplete pole figures of surface layers of AZ31 sheets rolled at 300–500 °C and small, moderate and large strain levels

intensity increases with the increase of the deformation strain and peaks at the intermediate temperature of 400 °C and small, moderate and large strain levels. Data obtained at nearly the same equivalent strain but different rolling temperatures are selected in this study to isolate the temperature effect on the (0002) rolling texture. Changes in the (0002) pole intensity with the starting rolling temperature are shown in Fig. 6. The (0002) pole intensity increases from 300 to 400 °C and sharply decreases with further increase in rolling temperature at each strain level. The sharpest decrease in the (0002) pole intensity is found at the largest strain level of approximately 1.4, although the rolling temperatures between the two samples differ by only 50 °C. Therefore, it is worthwhile to examine the microtexture and microstructure of the two samples rolled at 400 and 450 °C.

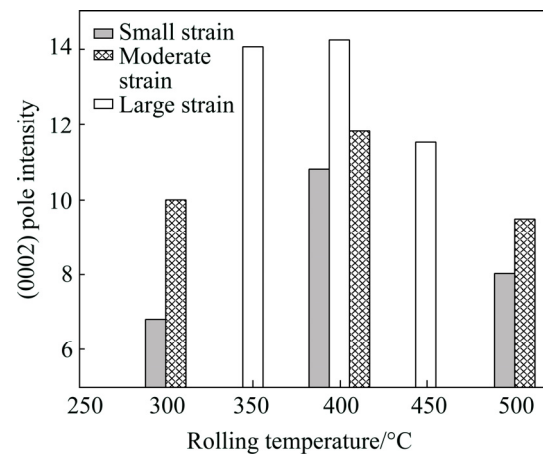


Fig. 6 (0002) pole intensity vs rolling temperature at small, moderate and large strain levels

The (0002) and $(10\bar{1}0)$ pole figures of AZ31 alloys rolled at 400 and 450 °C with 39% reduction measured by EBSD are shown in Figs. 7(a) and (b), respectively. The (0002) basal texture component spreading at 30°–40° away from ND to TD is observed in the 450 °C rolled sample. This result is in good agreement with the macrot texture measured by XRD, shown in Fig. 5. However, in the sample rolled at 400 °C, the (0002) basal pole is accumulated in the range of less than 30° with respect to ND. Such texture change and its relationship with the microstructural evolution are discussed as follows. We determine the possibility that DRX, mechanical twinning, and non-basal slip could cause the weakening (0002) basal texture intensity at high rolling temperature. Firstly, the influence of DRX on the texture evolution is examined. The new grains from DRX have basal planes rotated 30°–40° away from the rolling plane [16,17]. Thus, improving the DRX fraction can scatter the (0002) basal intensity to some extent. Figures 7(c) and (d) present the OIM grain

boundary maps of AZ31 alloy rolled at 400, 450 °C with 39% reductions, respectively. No differences in the DRX fractions are found between the samples rolled at 400 and 450 °C. The high angle grain boundary (HAGB) fractions of the samples processed at 400 °C, 450 °C and 39% reduction are 69.6% and 65%, respectively (Table 1). These parameters demonstrate that texture randomization may not be attributed to DRX fraction at high rolling temperature. Microstructures obtained from samples rolled up to medium strain level are also examined.

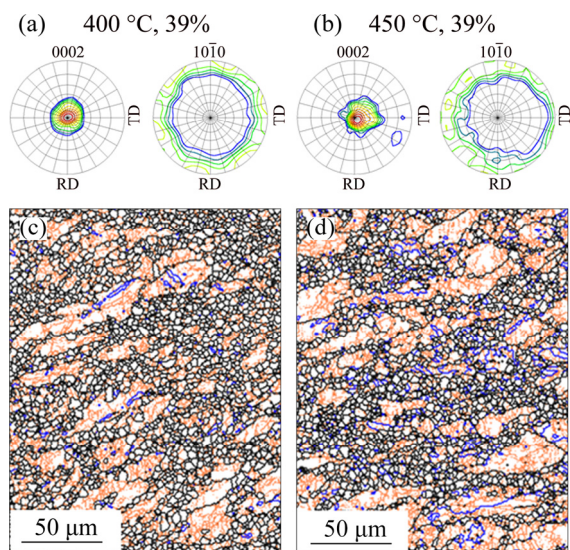


Fig. 7 (0002) and $(10\bar{1}0)$ pole figures of AZ31 alloys rolled at 400 °C (a) and 450 °C (b) with 39% reduction, and OIM grain boundary maps of AZ31 alloy rolled at 400 °C (c) and 450 °C (d) with 39% reduction

Figure 8 shows the optical micrographs of the surface layer of AZ31 alloy rolled to the medium strain level of approximately 0.8 at 300, 400 and 500 °C with 35% reduction. The number of DRX grains and the DRX grain size apparently differ among the three optical micrographs. A small number of DRX grains are observed in the samples rolled at 300 °C and 500 °C (Figs. 8(a) and (c), respectively), contrary to the large number of DRX grains in the sample rolled at 400 °C (Fig. 8(b)). Therefore, DRX fraction is not responsible for the reduced (0002) basal texture intensity of AZ31 alloys at high rolling temperatures. The sheet rolled at high temperature does not result in a larger fraction of DRX because of the following factors which may be related to the dynamic recovery (DRV) mechanism at high rolling temperatures. An increased level of DRV has been reported with increasing rolling temperatures in AZ31 magnesium alloys [18]. DRV and DRX are competing processes because both are driven by the energy stored during deformation [19]. Once DRX occurred and the deformation substructure was consumed, no further recovery could then occur.

Consequently, at 500 °C rolling, DRV consumed more stored energy during deformation, which led to decreasing fraction of DRX. The fractions of rolling temperature and strain are two dominant factors for DRX and DRV. Hence, the temperature becomes an important factor when the rolling strain is almost at the same level. Consequently, a decrease in DRX at high rolling temperature can be expected.

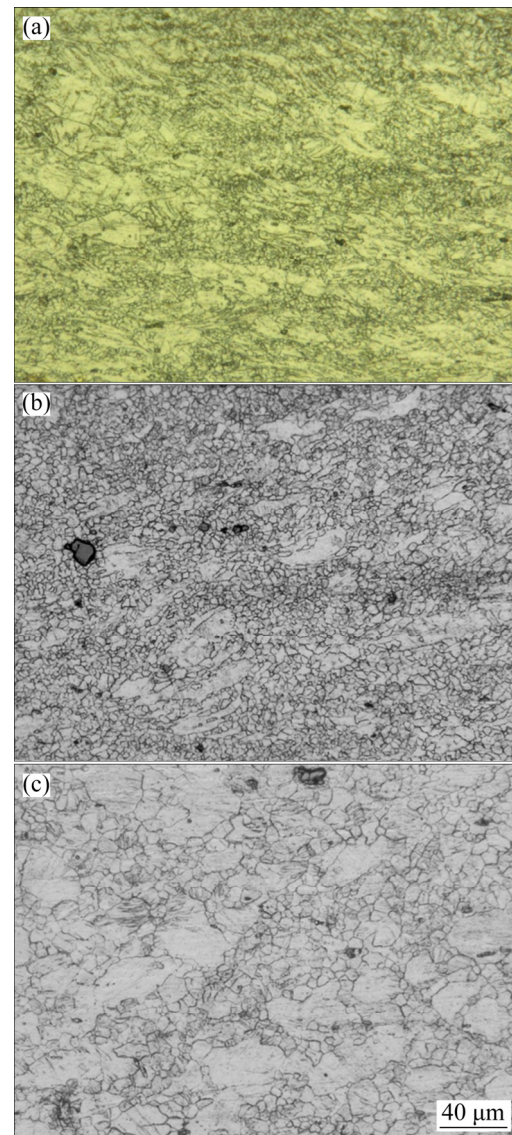


Fig. 8 Optical micrographs of surface layer of AZ31 alloy rolled at 300 °C (a), 400 °C (b) and 500 °C (c) with 35% reduction

Furthermore, an average misorientation between each pair of neighboring grains is calculated in the range of 0° to 70° (excluding the 86° mechanical twin). The results are listed in Table 1. The average misorientation angles of 400 °C and 450 °C rolled samples are 27.6° and 25.8°, respectively. Little difference is found between the two samples, confirming that DRX is not the main cause of the weakening (0002) basal texture.

Table 1 Comparison of microstructure parameters of samples rolled at 400 °C and 450 °C with 39% reduction

Rolling temperature/ °C	Equivalent strain	Twin boundary fraction/%	HAGB/%	Average misorientation angle, θ (°)
400	1.42	3.7	69.6	27.6
450	1.37	7.1	65.0	25.8

3.3 Effect of twinning on (0002) rolling texture

Twinning deformation modes play an important role in the deformation of hexagonal magnesium because of the limited number of slip systems for dislocation slip. $\{10\bar{1}2\}\langle 10\bar{1}1 \rangle$ ($86.3^\circ \langle 11\bar{2}0 \rangle$) twin is easily activated by the c -axis tension because of a lower critical resolved shear stress (CRSS). This kind of twinning reorients the c -axis of the twin nearly parallel to the compression axis [20], contributing to the weakening of the basal texture. The ($86.3^\circ \pm 15^\circ$) $\langle 11\bar{2}0 \rangle$ twin boundaries and their fractions are analyzed by EBSD (Figs. 9(a) and (b)). The $\{10\bar{1}2\}\langle 10\bar{1}1 \rangle$ twinned grains and their accompanying crystal orientations in (0001) crystallographic texture are shown and highlighted by black color in Fig. 9(c). The twinned grains change the orientation of the rolled grains and scatter the (0001) basal textures. The twin boundary fraction of the sample rolled at 450 °C is 7.1%, approximately twice as much as that of the sample rolled at 400 °C (3.7%). Thus, the larger fraction of $86.3^\circ \langle 11\bar{2}0 \rangle$ mechanical twinning is one reason for the reduced (0002) basal pole intensity.

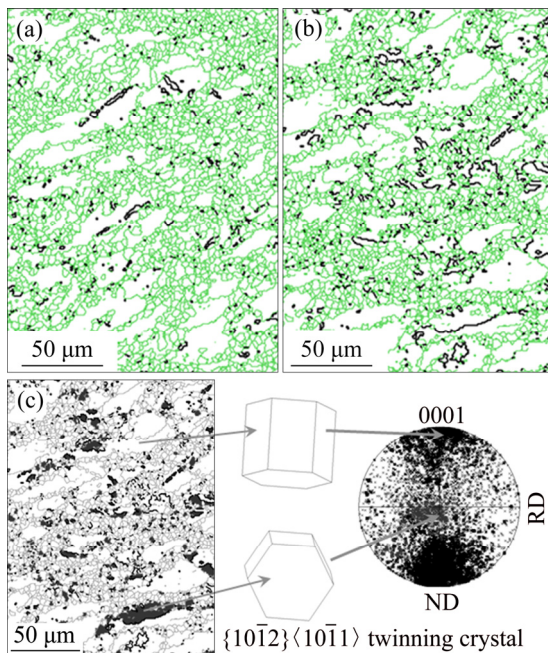


Fig. 9 ($86.3^\circ \pm 15^\circ$) $\langle 11\bar{2}0 \rangle$ twin boundary maps (marked as black lines) of AZ31 alloy rolled at 400 °C (a), 450 °C (b) with 39% reduction, and twinned grains and accompanying crystal rotations in (0001) pole figure (c) analyzed by EBSD

However, this result may be disputed because mechanical twinning occurs easily at low-temperature deformation because twinning has lower threshold stress than $\langle c+a \rangle$ slip in the temperature range of 100–200 °C. Nevertheless, mechanical twinning is also strongly influenced by initial grain size. Previous experimental results show that twinning is easier to operate at larger grain sizes [21]. Therefore, the lower (0002) basal texture intensity found in the current work is most likely due to the fact that larger grain size at high temperature rolling results in higher activation of mechanical twinning.

The CRSS for non-basal slip systems of prismatic $\langle a \rangle$ slip and pyramidal $(11\bar{2}2)\langle \bar{1}\bar{1}23 \rangle$ $\langle c+a \rangle$ slip decreases markedly when the deformation temperature is higher than 400 °C. Thus, non-basal slip systems are operated easily at high temperature rolling which can reduce (0002) basal texture intensity. Several studies have shown that the main component of texture 33° – 38° away from the basal pole is observed in samples deformed at high temperature and low strain compression [22]. This phenomenon is also attributed to the change in the activation balance between the basal and non-basal slip systems. Previous work studied the role of non-basal slip in magnesium alloy AZ31B by computer simulation using a viscoplastic self-consistent model [23,24]. The polycrystal simulation results indicate that an increased activity of non-basal $\langle c+a \rangle$ dislocation provides a self-consistent explanation for the observed changes in the anisotropy with increasing temperature. Thus, the increased activity of non-basal $\langle c+a \rangle$ slip systems at high temperature rolling may be responsible for the weakening of the (0002) basal texture.

In summary, the weakening of the (0002) basal texture at high temperature rolling may be attributed to two factors, namely, the activation of $86.3^\circ \langle 11\bar{2}0 \rangle$ mechanical twinning and the operation of non-basal slip systems. Rolling temperature can strongly influence the DRX fraction under similar equivalent strain. However, the results from the current study show very slight effect of DRX on the weakening of the (0002) texture intensity.

3.4 Temperature–strain dependency of as-rolled AZ31 texture

The simultaneous influence of temperature and equivalent strain on the basal texture intensity during hot rolling process is examined. The temperature history in the roll bite is more important than the starting rolling temperature because of its strong influence on deformation microstructures. Thus, the average rolling temperature is used here [11]. Figure 10 presents the contour map of the (0002) basal texture intensity in the surface layer. The (0002) texture intensity increases with

the increase of equivalent strain. Therefore, rolled sheets with weaker (0002) basal texture intensity are obtained at lower strain levels. In addition, the (0002) basal texture intensity peaks in the middle temperature range of 250–320 °C when the samples were rolled up to the largest strain level of 1.1–1.4. However, higher (0002) basal texture intensity is unexpected. Thus, lower rolling reductions and an appropriate average temperature range (higher than 370 °C or lower than 270 °C) are needed to obtain rolled sheets with the weakest (0002) basal texture intensity.

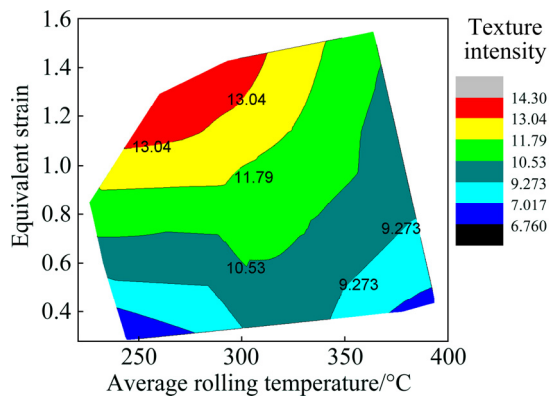


Fig. 10 Contour map of (0002) basal texture intensity in surface layer

4 Conclusions

1) The (0002) pole intensity of the surface layers increases as equivalent strain increases, contrary to the slightly decreasing (0002) basal texture intensity in the center layers with the rolling reduction. This phenomenon is most likely due to different deformation modes between the surface and center layers.

2) The highest (0002) pole intensity is found at rolling temperature of 400 °C. Then, the intensity decreases sharply with increasing rolling temperature. Analyses of the microstructures at different rolling temperatures but the same equivalent strain indicate that the reduced intensity is caused by the activation of the 86.3° $\langle 11\bar{2}0 \rangle$ mechanical twinning and operation of non-basal slip systems.

3) The optical microstructures and textures at various rolling temperatures but almost in the same strain levels are also examined. The results clearly show the very slight effect of DRX on the weakening of the (0002) texture intensity.

4) The optimum rolling conditions to obtain rolled sheets with the weakest (0002) basal texture intensity are derived from the temperature–strain dependency map. These conditions are low equivalent strain ranges (<0.6) and an appropriate temperature higher than 370 °C or

lower than 270 °C.

Acknowledgments

Project title: Microstructure simulation of AZ31 magnesium alloys during hot rolling based on a model of dislocation density. The experimental work was supported partly by Fujita Laboratory in the Department of Metallurgy, Tohoku University of Japan.

References

- [1] ZHOU Ping, BEEH ELMAR, WANG Meng, FRIEDRICH HORST E. Dynamic tensile behaviors of AZ31B magnesium alloy processed by twin-roll casting and sequential hot rolling [J]. Transactions of Nonferrous Metals Society of China, 2016, 26: 2846–2856.
- [2] WANG Hai-lu, WANG Guo-jun, HU Lian-xi, WANG Qiang, WANG Er-de. Effect of hot rolling on grain refining and mechanical properties of AZ40 magnesium alloy [J]. Transactions of Nonferrous Metals Society of China, 2011, 21: 229–234.
- [3] TADANO Y. Formability of magnesium sheet with rolling texture [J]. International Journal of Mechanical Sciences, 2016, 108–109: 72–82.
- [4] CHO Jae-Hyung, JEONG Sang-Soo, KIM Hyoung-Wook, KANG Suk-Bong. Texture and microstructure evolution during the symmetric and asymmetric rolling of AZ31B magnesium alloys [J]. Material Science and Engineering A, 2013, 566: 40–46.
- [5] GUO Fei, ZHANG Ding-fei, FAN Xiao-wei, JIANG Lu-yao, YU Da-liang, PAN Fu-sheng. Deformation behavior of AZ31 Mg alloys sheet during large strain hot rolling process: A study on microstructure and texture evolutions of an intermediate-rolled sheet [J]. Journal of Alloys and Compounds, 2016, 663: 140–147.
- [6] CHINO Y, MABUCHI M, KISHIHARA R, HOSOKAWA H, YAMADA Y, WEN C E, SHIMOJIMA K, IWASAKI H. Mechanical properties and press formability at room temperature of AZ31 Mg alloy processed by single roller drive rolling [J]. Materials Transactions, 2002, 43: 2554–2560.
- [7] HUANG Xin-sheng, SUZUKI K, WATAZU A, SHIGEMATSU I, SAITO N. Microstructure and texture of Mg–Al–Zn alloy processed by differential speed rolling [J]. Journal of Alloys and Compounds, 2008, 457: 408–412.
- [8] AL-SAMMAN T, GOTTSTEIN G. Dynamic recrystallization during high temperature deformation of magnesium [J]. Material Science and Engineering A, 2008, 490: 411–420.
- [9] DEL-VALLE J A, PEREZ-PRADO M T, RUANO O A. Texture evolution during large-strain hot rolling of the Mg AZ61 alloy [J]. Material Science and Engineering A, 2003, 355: 68–78.
- [10] GUO Li-li, FUJITA F. Effect of equivalent strain and redundant shear strain on microstructure and texture evolution during hot rolling in Mg–3Al–1Zn alloys [J]. Journal of Material Science, 2012, 47: 6213–6219.
- [11] GUO Li-li, FUJITA F. Influence of rolling parameters on dynamically recrystallized microstructures in AZ31 magnesium alloy sheets [J]. Journal of Magnesium and Alloys, 2015, 3: 95–105.
- [12] HUANG Xin-sheng, SUZUKI K, WATAZU A, SHIGEMATSU I, SAITO N. Improvement of formability of Mg–Al–Zn alloy sheet at low temperatures using differential speed rolling [J]. Journal of Alloys and Compounds, 2009, 470: 263–268.
- [13] FLEISCHER R L. Single crystal lattice rotation during compression [J]. Journal of the Mechanics and Physics of Solids, 1958, 6(4): 301–306.
- [14] AGNEW S R, YOO M H, TOMÉ C N. Application of texture simulation to understanding mechanical behavior of Mg and solid

- solution alloys containing Li or Y [J]. *Acta Materialia*, 2001, 49: 4277–4289.
- [15] BEAUSIR B, BISWAS S, KIM D I, TOTTH L S, SUWAS S. Analysis of microstructure and texture evolution in pure magnesium during symmetric and asymmetric rolling [J]. *Acta Materialia*, 2009, 57: 5061–5077.
- [16] GALIYEV A, KAIBYSHEV R, GOTTSTEIN G. Correlation of plastic deformation and dynamic recrystallization in magnesium alloy ZK60 [J]. *Acta Materialia*, 2001, 49: 1199–1207.
- [17] MA R, WANG L, WANG Y N, ZHOU D Z. Microstructure and mechanical properties of the AZ31 magnesium alloy sheets processed by asymmetric reduction rolling [J]. *Materials Science and Engineering A*, 2015, 638: 190–196.
- [18] MYSHLYAEV M M, MCQUEEN H J, MWEMBELA A, KONOPLEVA E. Twinning, dynamic recovery and recrystallization in hot worked Mg–Al–Zn alloy [J]. *Materials Science and Engineering A*, 2002, 337: 121–133.
- [19] HMPHREYS F J, HATHERLY M. *Recrystallization and related annealing phenomena* [M]. 2nd ed. Amsterdam: Elsevier, 2004.
- [20] LIU Guo-dong, XIN Ren-long, SHU Xiao-gang, WANG Chun-peng, LIU Qing. The mechanism of twinning activation and variant selection in magnesium alloys dominated by slip deformation [J]. *Journal of Alloy and Compounds*, 2016, 687: 352–359.
- [21] JIANG M G, YAN H, CHEN R S. Twinning, recrystallization and texture development during multi-directional impact forging in an AZ61 Mg alloy [J]. *Journal of Alloys and Compounds*, 2015, 650: 399–409.
- [22] FAN Hai-dong, AUBRY S, ARSENLIS A, EL-AWADY JAAFAR A. Grain size effects on dislocation and twinning mediated plasticity in magnesium [J]. *Scripta Materialia*, 2016, 112: 50–53.
- [23] AGNEW S R, DUYGULU O. Plastic anisotropy and the role of non-basal slip in magnesium alloy AZ31B [J]. *International Journal of Plasticity*, 2005, 21: 1161–1193.
- [24] SHAO Yi-chuan, TANG Tao, LI Da-yong, ZHOU Guo-wei, ZHANG Shao-rui, PENG Ying-hong. Polycrystal modeling of hot extrusion texture of AZ80 magnesium alloy [J]. *Transactions of Nonferrous Metals Society of China*, 2016, 26: 1063–1072.

变形方式、动态再结晶和孪晶对 AZ31 镁合金轧制织构演变的影响

郭丽丽¹, Fumio FUJITA²

1. 大连交通大学 连续挤压工程研究中心, 大连 116028;

2. Department of Metallurgy, Graduate School of Engineering, Tohoku University, Aoba, Sendai, 980-8579, Japan

摘要: 为了获得 AZ31 镁合金轧制织构(0002)基面密度和轧制条件的定量关系, 在压下量为 20%~40%、轧制温度为 300~500 °C 的条件下对 AZ31 镁合金进行热轧试验。采用板材中嵌入镁合金圆柱的方法计算板材厚度方向的剪切应变和等效应变。利用光学金相显微镜、X 射线衍射和 EBSD 技术检测轧制板材的显微组织、表面层和中心层(0002)基面织构密度。定量分析应变、动态再结晶和孪晶对 AZ31 镁合金轧制板材织构的影响。结果表明: 在相同应变下, 轧制开始温度为 400 °C 时, (0002)基面织构极密度最高, 并得到了(0002)基面织构极密度随温度和应变的变化规律。

关键词: 镁合金板材; 热轧; 织构; 动态再结晶; 孪晶

(Edited by Wei-ping CHEN)